Pergamon

0277-5387(95)00098-4

Polyhedron Vol. 14, No. 20–21, pp. 3067–3076, 1995

0277-5387/95 $9.50+0.00

SYNTHESIS, CHARACTERIZATION AND REACTIVITY OF LANTHANIDE(II) POLY(PYRAZOL-1-YL)BORATES (Ln = Sm, Eu AND Yb); FLUORESCENCE STUDIES OF $[EuL_2(THF)_2]$ [L = $B(pz)_4$, $HB(pz)_3$]; X-RAY CRYSTAL STRUCTURES OF $[Eu\{B(pz)_4\}_2(THF)_2]$ AND $[Yb\{B(pz)_4\}_3]\cdot C_2H_5OH$

ÂNGELA DOMINGOS, JOAQUIM MARÇALO, NOÉMIA MARQUES† and A. PIRES DE MATOS

Departamento de Química, ICEN/INETI, 2686 Sacavém Codex, Portugal

and

ADELINO GALVÃO

C. Q. E., Complexo 1, Instituto Superior Técnico, Av. Rovisco Pais 1096 Lisboa Codex, Portugal

and

P. C. ISOLANI, G. VICENTINI and K. ZINNER

Instituto de Química, Universidade de São Paulo, P.O. Box 20780, São Paulo 01498-970, Brazil

(*Received* 10 *January* 1995; *accepted* 20 *February* 1995)

Abstract—The reaction $[LnI_2(THF)_x]$ (Ln = Sm, Eu, Yb) with 2 equiv. of $K[B(pz)_4]$ (pz = pyrazolyl) in THF resulted in the formation of $[Ln\{B(pz)_4\}_2(THF)_2]$ complexes. The molecular structure of $[Eu\{B(pz)_4\}_2(THF)_2]$ has been determined by single-crystal X-ray diffraction analysis. The $[Sm\{B(pz)_4\}_2(THF)_2]$ and $[Yb\{B(pz)_4\}_2(THF)_2]$ complexes are fluxional in solution, as indicated by the equivalence of the pyrazolyl rings in the ^1H NMR spectra at room temperature. A static spectrum could be obtained for the Sm compound at −68°C with a pattern that is in accordance with the geometry found for the Eu complex, in the solid state. The complexes $[Ln\{HB(pz)_3\}_2(THF)_2]$ (Ln = Sm, Eu, Yb) have been prepared by the procedure used to synthesize the $[Ln\{B(pz)_4\}_2(THF)_2]$ complexes. The THF molecules can be replaced by 1,2-dimethoxyethane yielding the compounds $[Ln\{HB(pz)_3\}_2(DME)]$ (Ln = Sm, Yb). $[Sm\{B(pz)_4\}_2(THF)_2]$ and $[Yb\{B(pz)_4\}_2(THF)_2]$ react readily with alkyl halides, alcohols or alkynes to yield Ln^{III} complexes that disproportionate to the $[Ln\{B(pz)_4\}_3]$ complexes. The crystal structure of the compound $[Yb\{B(pz)_4\}_3]\cdot C_2H_5OH$ obtained in the reaction of $[Yb\{B(pz)_4\}_2(THF)_2]$ with ethanol was determined by X-ray diffraction analysis. Fluorescence studies on the Eu compounds are also reported.

Ever since their preparation by Trofimenko, the poly(pyrazolyl)borates have found extensive use as chelating ligands in *d*- and *f*-transition-metal chemistry. Several lanthanide(III) compounds have been described[1–21] but the reports concerning lanthanides in the +2 oxidation state are scarce. Lanthanide(II) compounds of Sm, Eu and Yb with $[HB(pz)_3]^-$ and $[HB(3,5\text{-}Me_2pz)_3]^-$ have been prepared by metathesis reactions of the lanthanide dihalides with the

†Author to whom correspondence should be addressed.

potassium salts of the ligands, in the stoichiometric ratio 1:2,[17,18,22-25] and the structural characterizations of $[Sm\{HB(3,5\text{-}Me_2pz)_3\}_2]$[18] and $[Yb\{HB(3,5\text{-}Me_2pz)_3\}_2]$[17] have also been carried out. The bis-ligand complexes, $[Ln\{HB(3\text{-}Rpz)_3\}_2]$ (Ln = Sm, Yb; R = Ph, 2′-thienyl),[24] the "half-sandwich" complexes $[Ln\{HB(3\text{-}Bu^t,5\text{-}Mepz)_3\}I(THF)_x]$ (Ln = Sm, $x = 2$; Yb, $x = 1$), as well as the derivatives $[Yb\{HB(3\text{-}Bu^t,5\text{-}Mepz)_3\}ER]$ [ER = $HBEt_3$, $N(SiMe_3)_2$, C≡CPh, CH_2SiMe_3, $CH(SiMe_3)_2$] were also reported.[24,25] Our interest in these complexes is due to the known reducing power of lanthanide (II) complexes and its application on synthetic chemistry.[26] In this contribution, we report on the synthesis and characterization of the lanthanide(II) complexes $[Ln\{B(pz)_4\}_2(THF)_2]$ and $[Ln\{HB(pz)_3\}_2 \cdot 2S]$ (S = THF, 1/2 DME).

The compounds synthesized were characterized by IR and ^1H NMR spectroscopies and by FTICR mass spectrometry. X-ray diffraction analysis were made on $[Eu\{B(pz)_4\}_2(THF)_2]$ and $[Yb\{B(pz)_4\}_3]$ compounds. Fluorescence spectra and their behaviour as a function of temperature were also studied for the Eu compounds.

EXPERIMENTAL

General procedure

All operations were carried out under argon using glovebox, Schlenk and vacuum-line techniques. Solvents (THF, benzene, benzene-d_6, toluene, toluene-d_8, hexane) were purified by distillation from sodium benzophenone ketyl and degassed immediately before use. $K[HB(pz)_3]$ and $K[B(pz)_4]$ were prepared as described previously.[27] The THF solutions of the lanthanide diiodides were prepared according to literature procedures.[28] ^1H NMR spectra were recorded using a Bruker SY80FT multinuclear spectrometer and the proton chemical shifts are reported in ppm relative to Me_4Si. IR spectra were recorded on a Perkin–Elmer 577 spectrophotometer using Nujol mulls between CsI plates. Carbon, hydrogen and nitrogen analyses were performed on a Perkin–Elmer automatic analyser.[29] The FTICR mass spectra were obtained by laser desorption (LD), with an Extrel FTMS (Waters) Model 2001-DT spectrometer equipped with a 3.0 T superconducting magnet and interfaced to a Spectra-Physics Quanta-Ray GCR-11 pulsed Nd : YAG laser operating at the fundamental wavelength (1064 nm) with an estimated output of 20–50 mJ per pulse following a previously described technique.[30] Fluorescence spectra were recorded on a Hitachi Perkin–Elmer MPF-4 spectrofluorimeter, with modifications for solid samples positioning and thermostating at low temperatures.[31]

Synthesis and characterization

$[Sm\{B(pz)_4\}_2(THF)_2]$ (**1**). $K[B(pz)_4]$ (460 mg, 1.45 mmol) was added to a solution (0.04 M) of SmI_2 in THF (0.72 mmol). After addition the deep blue solution turned almost immediately brown. After stirring for 16 h, the solution was separated from the KI precipitate by centrifugation, and was evaporated to dryness. The brown compound was obtained in 75% yield (389 mg, 0.54 mmol). IR [Nujol mulls, ν (cm^{-1})]: 1504 s, 1462 s, 1420 s, 1380 s, 1289 s, 1212 s, 1186 s, 1095 s, 1050 s, 978 m, 915 m, 881 w, 835 sh, 800 s, 758 s, 670 w, 620 m, 340 m. ^1H NMR 303 K [C_7D_8, δ (ppm)]: 8.25, 6.6 (v br), 4.98 (v br), 3.42 (8H, α-CH_2, THF), 1.36 (8H, β-CH_2, THF). FTICR/MS (*m/z* referenced to the species ^{152}Sm and ^{11}B; relative abundance in parentheses): LD(+) 710 (55%) [M^+]; 642 (26%) [M^+-pzH]; 498 (34%) [M^+-Bpz_3]; 430 (29%) [M^+-Bpz_4H]; 152 (100%) [Sm^+].

$[Eu\{B(pz)_4\}_2(THF)_2]$ (**2**). The orange europium compound (323 mg, 0.38 mmol, 80% yield) was obtained by the same procedure. IR [Nujol mulls, ν (cm^{-1})]: 1504 s, 1462 s, 1420 s, 1379 s, 1290 s, 1214 s, 1187 s, 1095 s, 1053 s, 978 m, 919 m, 883 w, 847 sh, 800 s, 761 s, 672 w, 621 m, 340 m. FTICR/MS (*m/z* referenced to the species ^{153}Eu and ^{11}B; relative abundance in parentheses): LD(+) 711 (18%) [M^+]; 643 (15%) [M^+-pzH]; 153 (100%) [Eu^+].

$[Yb\{B(pz)_4\}_2(THF)_2]$ (**3**). The brick red ytterbium compound (337 mg, 0.38 mmol, 80% yield) was obtained as described for **1**. IR [Nujol mulls, ν (cm^{-1})]: 1502 s, 1463 s, 1420 s, 1381 s, 1291 s, 1214 s, 1190 s, 1097 s, 1053 s, 976 m, 920 m, 890 w, 837 sh, 809 s, 758 s, 678 w, 620 m, 350 m. ^1H NMR [C_7D_8, δ (ppm)]: 7.74 (9H), 7.52 (9H), 5.98 (9H), 3.50 (8H, α-CH_2, THF), 1.38 (8H, β-CH_2, THF). FTICR/MS (*m/z* referenced to the species ^{174}Yb and ^{11}B; relative abundance in parentheses): LD(+) 732 (29%) [M^+]; 664 (15%) [M^+-pzH]; 520 (30%) [M^+-Bpz_3]; 174 (100%) [Yb^+].

$[Sm\{HB(pz)_3\}_2(THF)_2]$ (**4**). The compound was obtained as described for **1** by adding $K[HB(pz)_3]$ (354 mg, 1.40 mmol) to a solution (0.04 M) of SmI_2 in THF (0.70 mmol). The reddish-brown samarium compound was obtained with a yield of 80% (403 mg, 0.56 mmol). IR [Nujol mulls, ν (cm^{-1})]: 2449s, 1502 s, 1461 s, 1420 s, 1380 s, 1295 s, 1258 w, 1209 s, 1186 m, 1117 s, 1045 s, 969 m, 920 w, 884 m, 779 w, 756 s, 726 s, 667 m, 624 m, 329 m. ^1H NMR [C_7D_8, δ (ppm)]: 7.74 (6H), 7.52 (6H), 5.98 (6H), 3.50 (8H, α-CH_2, THF), 1.38 (8H, β-CH_2, THF).

FTICR/MS (*m/z* referenced to the species ^{152}Sm and ^{11}B; relative abundance in parentheses): LD(+) 578 (100%) [M^+]; 510 (7%) [M^+-pzH]; 432 (27%) [M^+-Bpz_2]; 152 (100%) [Sm^+].

[$Eu\{HB(pz)_3\}_2(THF)_2$] (**5**). The orange europium compound was obtained as described for the samarium compound in a yield of 75%. IR [Nujol mulls, ν (cm^{-1})]: 2450 s, 1502 s, 1460 s, 1410 s, 1380 s, 1295 s, 1212 s, 1190 m, 1120 s, 1045 s, 972 m, 920 w, 880 m, 778 s, 748 s, 730 s, 670 m, 625 m, 325 m. FTICR/MS (*m/z* referenced to the species ^{153}Eu and ^{11}B; relative abundance in parentheses): LD(+) 579 (100%) [M^+].

[$Yb\{HB(pz)_3\}_2(THF)_2$] (**6**). The deep-red ytterbium compound was synthesized as described for the above compound in a yield of 80%. IR [Nujol mulls, ν (cm^{-1})]: 2462 s, 1501 s, 1460 s, 1420 s, 1381 s, 1290 s, 1258 w, 1208 s, 1117 s, 1050 s, 967 w, 920 w, 801 w, 760 s, 723 s, 670 m, 617 m, 320 m. ^1H NMR [C_7D_8, δ (ppm)]: 7.71 (6H), 7.45 (6H), 6.03 (6H), 3.47 (8H,α-CH_2,THF), 1.43 (8H,β-CH_2,THF). FTICR/MS (*m/z* referenced to the species ^{174}Yb and ^{11}B; relative abundance in parentheses): LD(+) 600 (100%) [M^+]; 454 (14%) [M^+-Bpz_2]; 174 (%) [Yb^+].

[$Sm\{HB(pz)_3\}_2(DME)$] (**7**). The compound was obtained by dissolving **4** in dimethoxyethane and then evaporating the clear solution to dryness. IR [Nujol mulls, ν (cm^{-1})]: 2439 s, 1501 s, 1456 s, 1418 w, 1379 s, 1293 s, 1261 w, 1213 s, 1184 s, 1117 s, 1066 m, 1042 s, 967 m, 922 w, 880 w, 858 m, 799 m, 756 s, 724 s, 666 m, 626 m, 388 m, 332 m. ^1H NMR [C_7D_8, δ (ppm)]: 13.02 (6H), 10.07 (6H), −1.95 (6H), 4.14 (4H, CH_2,DME), −0.47 (6H, CH_3,DME). FTICR/MS (*m/z* referenced to the species ^{152}Sm and ^{11}B; relative abundance in parentheses): LD(+) 578 (100%) [M^+]; 432 (32%) [M^+-Bpz_2].

[$Yb\{HB(pz)_3\}_2(DME)$] (**8**). The analogous ytterbium compound was obtained by the same procedure. IR [Nujol mulls, ν (cm^{-1})]: 2454 s, 1503 s, 1456 s, 1420 m, 1376 s, 1297 s, 1259 m, 1212 s, 1184 s, 1114 vs, 1039 vs, 969 m, 917 m, 880 w, 806 sh, 800 s, 753 s, 720 s, 669 m, 622 m, 397 m, 326 m. ^1H NMR [C_7D_8, δ (ppm)]: 7.65 (6H), 7.37 (6H), 5.98 (6H), 3.29 (4H,CH_2,DME), 3.09 (6H,CH_3,DME).

X-ray crystallography of [$Eu\{B(pz)_4\}_2(THF)_2$] (**2**) and [$Yb\{B(pz)_4\}_3$]·C_2H_5OH (**9**)

Regular orange crystals of compound **2** were obtained by slow diffusion of n-hexane in a saturated solution of the complex in THF. Transparent white crystals of **9** were obtained by slow diffusion of n-hexane in a saturated solution of the product obtained in the reaction of [$Yb\{B(pz)_4\}_2(THF)_2$] with ethanol, in toluene. The crystals were mounted in quartz capillaries in an argon-filled glove-box and sealed under argon.

Data were collected at room temperature on an Enraf–Nonius CAD-4 diffractometer with graphite-monochromatized Mo-K_α radiation, using a ω–2θ scan mode. Unit-cell parameters were obtained by least-square refinement of the setting angles of 25 reflections with $17 < 2\theta < 30°$ for **2** and $21 < 2\theta < 32°$ for **9**. Details of the crystal, data collection and refinement are given in Table 1. Data were corrected for Lorentz–polarization, for linear

Table 1. Crystallographic data for compounds **2** and **9**

Compound	[$Eu\{B(pz)_4\}_2(THF)_2$ (**2**)	[$Yb\{B(pz)_4\}_3$·C_2H_5OH (**9**)
Formula	$C_{32}H_{40}B_2N_{16}O_2Eu$	$C_{38}H_{42}B_3N_{24}OYb$
Mol. wt	854.38	1056.39
Crystal system	Orthorhombic	Monoclinic
Space group	*Pnma*	$P2_1/c$
a (Å)	17.707(1)	14.663(6)
b (Å)	14.141(1)	13.755(1)
c (Å)	14.726(1)	23.312(9)
β (°)		106.49(2)
V (Å^3)	3687(1)	4508(3)
Z	4	4
D_{calc} (g cm^{-3})	1.539	1.556
Linear absorption coeff. (cm^{-1}) (Mo-K_α)	17.56	20.19
2θ range (°)	3.0–52.0	3.0–54.0
No. of reflections	3265[$I > 2\sigma(I)$]	7069[$F_o > 3\sigma(F_o)$]
Range in decay correction factors	———	1.00025–1.00221
Range in absorption correction factors	0.9397–0.9996	0.8335–0.9996
No. of parameters refined	295	415
Final *R*, R_w	0.050,0.115	0.061,0.074

decay for **9** and for absorption by empirical corrections based on Ψ scans, using the Enraf–Nonius program. The structures were solved by Patterson and Fourier methods.[32] For **2**, in the pyrazolyl N(2) that is at special position *m*, the atom C(22) was found to be disordered over three different positions and the atom C(23) over two positions. All non-hydrogen atoms were restrained to be isotropic within 0.005σ. Hydrogens were inserted at localized positions riding in the parent atom with an isotropic thermal motion parameter 20% higher than the equivalent for the parent atom. Full-matrix least-squares refinement[33] converged to $R_w = 0.115$ and $R_1 = 0.050$ $(w = 1/[\sigma^2(F_o^2) + (0.05P)^2 + 15.43P]$ where $P = [\max(F_o^2, 0) + 2F_c^2)/3]$; R_1 is the R factor for reflections with $I \geqslant 2\sigma(I)$. For **9** there is a lattice solvent molecule C_2H_5OH, partially disordered. It was accounted for by introducing one pair of oxygen atoms with partial occupancy. The carbon atoms also showed large thermal parameters giving in the refinement chemically unsatisfactory bond distances. All but the solvent and the carbon atoms of the molecule were refined anisotropically (due to the limit of the program on the number of atoms refined) by full-matrix least-squares procedures.[32] The contributions of the hydrogen atoms were included in calculated positions, constrained to ride on their carbon atoms with group U_{iso} values assigned. A weighting scheme $w = [\sigma(F_o^2) + 0.0015F_o^2]^{-1}$ was used. In the final difference Fourier map the highest peaks were 0.7 and 1.9 e $Å^{-3}$ for compounds **2** and **9** and were near the lanthanide atom. Calculations for structure **2** were carried out on an ALPHA 150 and for **9** on a Microvax 3400 at Instituto Superior Técnico. Atomic scattering factors and anomalous dispersion terms were taken from International Tables for X-ray Crystallography.[34]

RESULTS AND DISCUSSION

The reaction of 2 equiv. of $[B(pz)_4]^-$ with $[LnI_2(THF)_x]$ in THF resulted in the formation of $[Ln\{B(pz)_4\}_2(THF)_2]$ complexes [Ln = Sm (**1**), Eu (**2**) and Yb (**3**)] in good yield [eq. (1)].

$$[LnI_2(THF)_x] + 2K[B(pz)_4] \longrightarrow [Ln\{B(pz)_4\}_2(THF)_2] + 2KI \quad (1)$$

The complexes are soluble in THF and aromatic hydrocarbons and moderately soluble in saturated hydrocarbons. The europium complex is reasonably stable in solution but the other two, especially the samarium complex, decompose slowly in aromatic solvents.

Complexes $[Ln\{HB(pz)_3\}_2(THF)_2]$ [Ln = Sm (**4**), Eu (**5**) and Yb (**6**)] were prepared in a similar way. Compounds **5** and **6** could be sublimed at 150°C (10^{-3} mm Hg), but **4** decomposed when heated. The solubility of these complexes was similar to that found for Bpz_4 derivatives, but were less stable in solution. In one attempt to grow crystals for $[Yb\{HB(pz)_3\}_2(THF)_2]$, we have obtained $[Yb\{HB(pz)_3\}_3]$ whose crystal and molecular structure was already determined by Takats.[2] In this case a different crystalline form was obtained.[35] As the ^1H NMR spectrum of $[Sm\{HB(pz)_3\}_2(THF)_2]$ showed a complex dependence with temperature, we replaced the THF molecules by 1,2-dimethoxyethane, hoping to obtain a more rigid structure which would increase the energy barrier of the fluxional process, allowing us to obtain a static spectrum in the temperature range studied. This could be readily done by solubilizing the starting compound in dimethoxyethane followed by evaporation of the solvent. The compounds $[Ln\{HB(pz)_3\}_2(DME)]$ [Ln = Sm (**7**) and Yb (**8**)] were obtained.

The characterization of the complexes have been made on the basis of spectroscopic data and FTICR/MS.

Variable-temperature NMR studies

In solution, the Sm and Yb complexes undergo dynamic rearrangements that equilibrate all the pyrazolyl rings of the $[B(pz)_4]$ and $[HB(pz)_3]$ ligands. The ambient-temperature ^1H NMR spectrum of **1** in toluene-d_8 shows one resonance at 8.2 ppm and two other resonances almost collapsed at 6.6 and 5.0 ppm for each type of hydrogen atom in the pyrazolyl rings. The resonances at 3.4 and 1.4 ppm were assigned to the protons of the THF molecules. ^1H NMR studies at variable temperature allowed us to slow down the dynamic process and in the limiting static spectrum obtained at 210 K, nine signals were observed for the protons of the pyrazolyl rings at +10.4(1H), +8.8(1H), +8.6(2H), +8.4(2H), +7.0(1H), +6.8(1H), +6.7(1H), +4.6(2H) and −2.3 (1H) ppm, and +4.2 and +1.5 ppm for the THF protons. It was not possible to assign the pyrazolyl protons but three of them must be related to the protons of the uncoordinated pyrazole ring. Actually, fluxional behaviour due to exchange between the uncoordinated and the coordinated pyrazole rings has been extensively referred in the literature.[36] Moreover, the coordinated pyrazolyl rings show a splitting of 2 : 1 compatible with the solid-state structure found for $[Eu\{B(pz)_4\}_2(THF)_2]$ (see below). Although the X-ray structural analysis has only been undertaken for the Eu compound, it is reason-

able to assume that for Sm the structure is the same due to the similar ionic radii of the Sm and Eu ions. For $[Yb\{B(pz)_4\}_2(THF)_2]$ the ^1H NMR spectrum at room temperature presents three resonances for the protons of the pyrazolyl rings at +7.74, 7.52 and 5.98 ppm and two other resonances at 3.50 and 1.38 attributed to the protons of the THF. Line broadening of the resonances was observed upon lowering the temperature, but no static spectrum was observed.

For complex **4** the ^1H NMR spectrum at ambient temperature shows three resonances for the equivalent pyrazolyl rings of the tris(pyrazolyl)borate ligands and two resonances for the THF protons. At 250 K the resonances due to the $[HB(pz)_3]$ ligand were already collapsed, while the resonances of the THF remained sharp but a static spectrum was not obtained in the temperature range studied. Replacement of THF by DME did not increase significantly the barrier energy for the fluxional process as shown by the equivalence observed for the pyrazolyl groups of complex **7**, even at low temperature. For the Yb compounds **6** and **8** no static spectra could be obtained.

Crystal structure of $[Eu\{B(pz)_4\}_2(THF)_2]$ (**2**)

The crystal structure consists of discrete molecular units. Fig. 1 shows an ORTEP drawing of the molecule. The molecule contains a crystallographic-imposed mirror plane passing through Eu, B(1) and B(2) and the three pyrazolyl rings [N(2)···C(24), N(3)···C(34) and N(5)···C(54)]. The coordination geometry about europium is best described as approximately bicapped trigonal prismatic (BCTP; Fig. 2). The two $[B(pz)_4]^-$ ligands span one rectangular edge [N(1)—N(1′) and N(6)—N(6′)] and cap one rectangular face of the prism [pyrazolyl rings N(2) and N(5)]. The two oxygen atoms of the THF ligands span the other rectangular edge. The values of the shape parameters for the normalized polyhedron are listed in Table 2 along with the values for the idealized polyhedra.[37] The rectangular face of the prism [N(1)—N(1′)—O(1′)—O(1)] is effectively planar, and the triangular faces of the prism [N(1)—N(6)—O(1) and N(1′)—N(6′)—O(1′)] are inclined by 9.4°. The dihedral angle for the unique rectangular edge [N(6)—N(6′), 44.4°] is much larger than the value of 21.8° for the regular polyhedron.

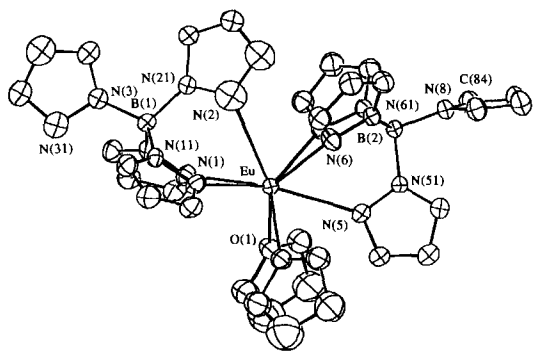

Fig. 1. ORTEP view of $[Eu\{B(pz)_4\}_2(THF)_2]$.

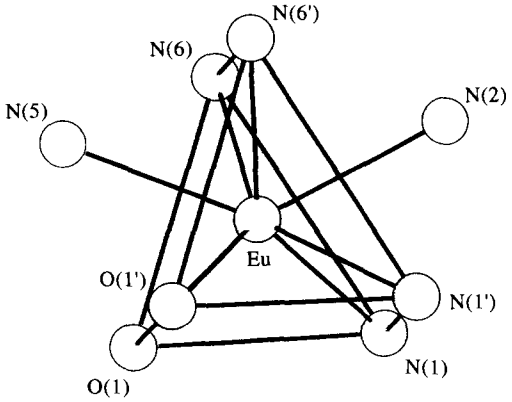

Fig. 2. BCTP coordination polyhedron of $[Eu\{B(pz)_4\}_2(THF)_2]$.

Selected bond distances and angles are given in Table 3. Bond length comparison with other related Eu^{II} complexes is difficult since no structures are known involving poly(pyrazolyl)borate ligands, but can be compared with samarium poly(pyrazolyl)borate complexes, since Eu^{II} and Sm^{II} show similar ionic radii. The Eu—N bond distances range from 2.661(8) to 2.77(2) Å with a mean value of 2.70 Å, which is longer than the value of 2.617(4) Å observed in the six-coordinate $[Sm\{HB(3,5\text{-}Me_2pz)_3\}_2]$ complex[18] and is in accordance with its higher coordination number. The Eu—O bond distance is 2.649(5) Å, which is close to the value of 2.64(2) Å observed in the eight-coordinate complex $Cp^*_2Sm(THF)_2$.[38] The O—Eu—O bond angle is 84.5(2)° and is comparable to the value of 82.6 (4)° found in $Cp^*_2Sm(THF)_2$.

FTICR/MS analysis

The positive ion Nd : YAG LD mass spectra were obtained for all the synthesized compounds and exhibit the molecular ion peaks LnL_2^+ ($[M^+]$) and different degrees of fragmentation, resulting from loss of pyrazolyl groups. Loss of THF and DME from the neutral parents was observed probably due to the lability of these ligands.

Table 2. Values of the δ and ϕ shape parameters for $[Eu\{B(pz)_4\}_2(THF)_2]$[a]

	n.p.	DOD	SAP	BCTP
δ N(2)[N(6)N(6′)]N(5)	44.4	29.5	0.0	21.8
δ N(1)[O(1)N(1′)]O(1′)	0.0	29.5	0.0	0.0
δ N(1)[N(6)O(1)]N(5)	48.1	29.5	52.4	48.2
δ N(1′)[N(6′)O(1′)]N(5)	48.1	29.5	52.4	48.2
δ N(2)[N(1)N(6)]O(1)	37.2	29.5	52.4	48.2
δ N(2)[N(1′)N(6′)]O(1′)	37.2	29.5	52.4	48.2
ϕ N(6)—N(5)—O(1′)—N(1)	7.0	0.0	24.5	14.1
ϕ N(6′)—N(2)—N(1)—O(1)	12.5	0.0	24.5	14.1

[a] n.p. = normalized polyhedron, DOD = dodecahedron, SAP = square antiprism and BCTP = bicapped trigonal prism.

Table 3. Selected bond distances (Å) and angles (°) for $[Eu\{B(pz)_4\}_2(THF)_2]$

Eu—N(1)	2.698(6)	Eu—N(6)	2.677(6)
Eu—N(2)	2.77(2)	Eu—O(1)	2.649(5)
Eu—N(5)	2.661(8)		
N(1)—Eu—N(6)	94.2(2)	N(6)—Eu—N(6)[a]	76.1(2)
N(1)—Eu—O(1)	73.8(2)	O(1)—Eu—O(1)[a]	84.5(2)
N(6)—Eu—O(1)	86.9(2)	N(2)—Eu—N(5)	131.0(4)
N(1)—Eu—N(1)[a]	70.2(3)		
N(2)—Eu—N(1)	67.0(3)	N(5)—Eu—O(1)	73.4(2)
N(2)—Eu—N(6)	74.4(3)	N(5)—Eu—N(6)	67.5(2)

[a] Atoms related by the symmetry operation $x, -y+0.5, z$.

Fluorescence studies

The fluorescence spectrum of $[Eu\{B(pz)_4\}_2(THF)_2]$ shows a weak band with a maximum at 465 nm, very similar to $[EuI_2(THF)_2]$ which presents a narrow band with a maximum at 470 nm. The fluorescence spectrum of $[Eu\{HB(pz)_3\}_2(THF)_2]$ at room temperature displays an intense, broad band with a maximum at 586 nm. This band shows no fine structure, therefore seeming to contain no structural information. Excitation of fluorescence at 370 or 395 nm does not alter the emission spectra. The excitation band is very broad, extending from 285 to *ca* 500 nm. The ligand $K[HB(pz)_3]$ is very weakly fluorescent in the range 360–390 nm, near the detection limit of our instrumentation.

The fluorescence spectrum of $[Eu\{HB(pz)_3\}_2(THF)_2]$ in liquid nitrogen (77 K) shows a not significantly different band (with respect to room temperature) with a maximum at 607 nm and without any significant change in emission intensity.

The investigation of fluorescence as a function of temperature shows almost no difference in band width or shape. In order to evaluate the wavelength shift, spectra from 80 to 300 K were recorded and the intensities at 560 and 620 nm measured.

A plot of ln(I560/I620) vs $1/T$ (1/K) is shown in Fig. 3. This plot reproducibly shows two straight lines with a transition point at 238 K (−35°C), suggesting a phase transition at this temperature.

This behaviour of fluorescence with temperature may be due to vibrational freezing of the upper electronic level responsible for this emission, thus lowering its energy and causing this wavelength shift to the red. The very small fluorescence intensity of $[Eu\{B(pz)_4\}_2(THF)_2]$ may be due to the fourth (non-coordinated) pyrazolyl ring, where vibrations or even restricted rotations (in the solid state) may be a very efficient internal conversion channel, thus lowering the fluorescence quantum yield.

We look forward to performing X-ray analysis in $[Eu\{HB(pz)_3\}_2(THF)_2]$ at different temperatures in order to establish a relationship between structure and this behaviour of fluorescence.

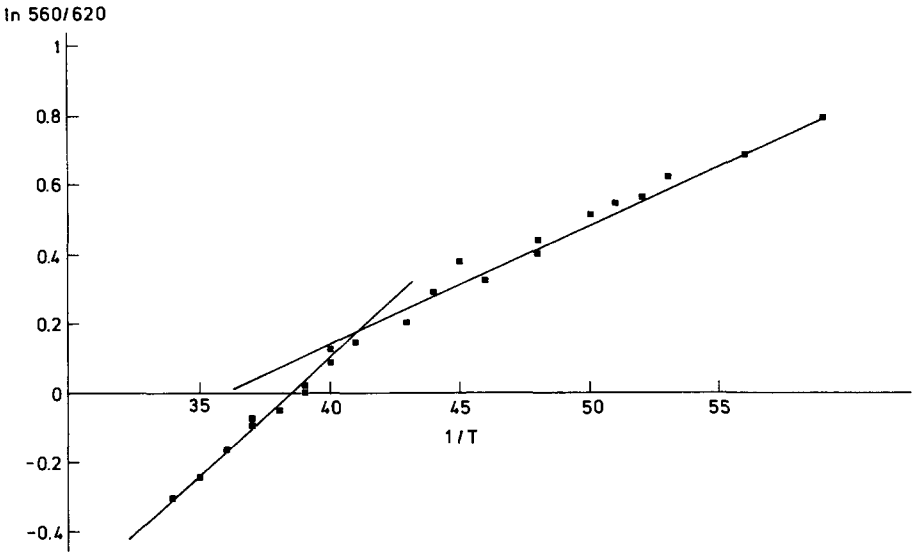

Fig. 3. Arrhenius plot of ln (I560/I620) as a function of $1/T$ (1/K).

Reactivity studies

The $[Sm\{B(pz)_4\}_2(THF)_2]$ and $[Yb\{B(pz)_4\}_2(THF)_2]$ complexes undergo fast electron-transfer reactions with alkyl halides, alcohols or alkynes to yield products that we were not able to characterize properly. Recrystallization from a toluene/hexane solution of the compound obtained when ethanol reacted with $[Yb\{B(pz)_4\}_2(THF)_2]$ yielded white transparent crystals suitable for X-ray diffraction analysis. The compound proved to be $[Yb\{B(pz)_4\}_3]\cdot C_2H_5OH$ (**9**) due to disproportionation of the Yb^{III} compound formed in the reaction.† This type of rearrangement was also observed during the recrystallization process of $[Yb\{HB(pz)_3\}_2(DME)]$ which yielded the previously reported $[Yb\{HB(pz)_3\}_3]$,[2] as mentioned above.

Crystal structure of $[Yb\{B(pz)_4\}_3]\cdot C_2H_5OH$ (**9**)

The crystal structure consists of discrete molecular units. An ORTEP view of the molecule is shown in Fig. 4. The structure shows that the ytterbium ion is eight-coordinate with two tridentate and one bidentate $[B(pz)_4]^-$ ligands. The result is similar to that reported by Takats *et al.*[2] for $[Yb\{HB(pz)_3\}_3]$.

The molecule has an approximate plane of symmetry containing the ytterbium atom, the three boron atoms and three pyrazolyl rings [N(1)···C(13), N(5)···C(53) and N(12)···C(123)].

The coordination geometry about the ytterbium is best described as a bicapped trigonal prism (Fig. 5). Both tridentate $[B(pz)_4]^-$ ligands span one rectangular edge [N(2)—N(3) and N(6)—N(7)] and cap one rectangular face of the prism [pyrazolyl rings N(1) and N(5)]. The bidentate ligand spans the remaining rectangular edge, N(9)—N(10). The values of the shape parameters for the normalized polyhedron[37] are listed in Table 4, along with the values for the idealized polyhedra. The rectangular face of the prism [N(2)—N(3)—N(10)—N(9)] is approximately planar with a δ value of 7.3°. The effect of the capping atoms N(1) and N(5) in elongating the triangular edges of the capped rectangular faces led to a δ value for the unique rectangular edge, N(6)N(7), of 39.2°, much larger than the value of 21.8° for the idealized polyhedron. The triangular top and bottom faces of the prism [N(3)—N(6)—N(10) and N(2)—N(7)—N(9)] are inclined by 4.6°.

Selected bond distances and bond angles are listed in Table 5. The Yb—N bond distances range from 2.379(8) to 2.596(9) Å with a mean value of 2.47 Å, the longest Yb—N bond lengths being associated with the capping nitrogen atoms. The

†The X-ray structural analysis of a colourless crystal of the analogous samarium complex, obtained also by disproportionation of the compound formed in the reaction of $[Sm\{B(pz)_4\}_2(THF)_2]$ with ethanol [crystal data: $P2_1/n$, $Z = 4$, $a = 17.858(11)$, $b = 13.436(3)$, $c = 20.988(11)$ Å, $\beta = 109.10(2)°$, $V = 4759(4)$ Å^3], revealed a similar structure to that of the Yb derivative. Although the ionic radius of Sm^{3+} is larger than that of the Yb^{3+} ion, the metal centre is still eight-coordinate with the same geometry.

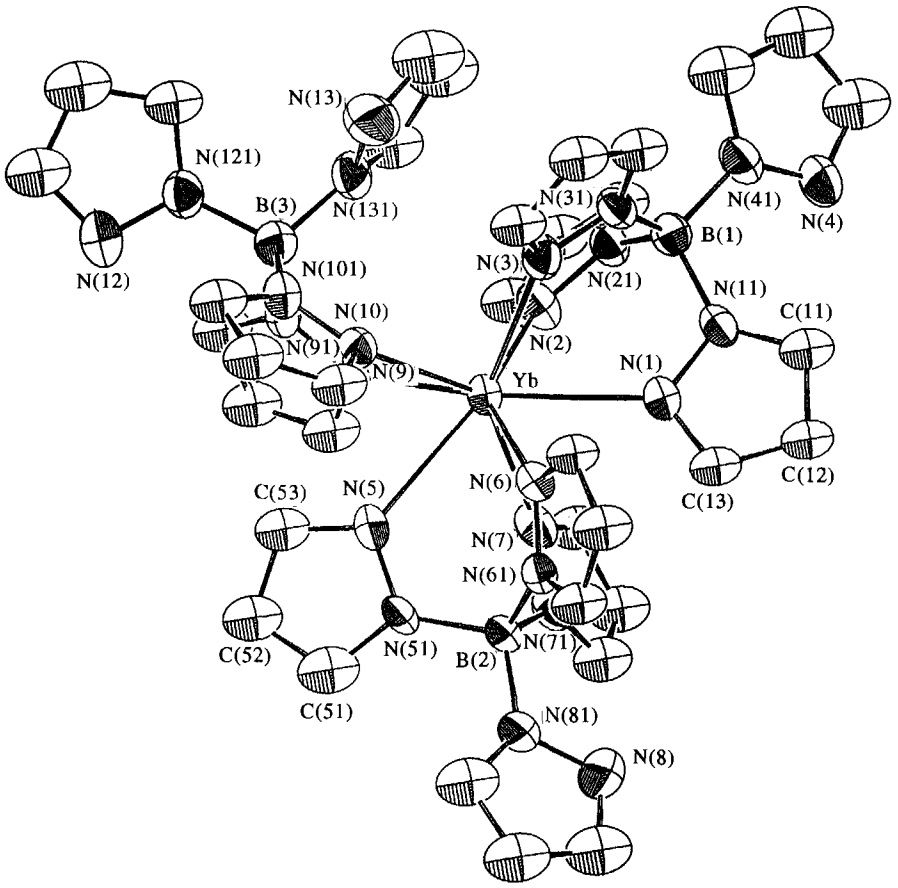

Fig. 4. ORTEP view of $[Yb\{B(pz)_4\}_3]$.

Table 4. Values of the δ and ϕ shape parameters for $[Yb\{B(pz)_4\}_3]$[a]

	n.p.	DOD	SAP	BCTP
δ N(1)[N(6)N(7)]N(5)	39.2	29.5	0.0	21.8
δ N(2)[N(3)N(9)]N(10)	7.3	29.5	0.0	0.0
δ N(2)[N(7)N(9)]N(5)	39.7	29.5	52.4	48.2
δ N(3)[N(6)N(10)]N(5)	46.1	29.5	52.4	48.2
δ N(1)[N(7)N(2)]N(9)	48.3	29.5	52.4	48.2
δ N(1)[N(6)N(3)]N(10)	42.5	29.5	52.4	48.2
ϕ N(6)—N(5)—N(9)—N(2)	16.0	0.0	24.5	14.1
ϕ N(7)—N(1)—N(3)—N(10)	13.9	0.0	24.5	14.1
ϕ N(6)—N(1)—N(2)—N(9)	7.9	0.0	24.5	14.1
ϕ N(7)—N(5)—N(10)—N(3)	10.2	0.0	24.5	14.1

[a] n.p. = normalized polyhedron, DOD = dodecahedron, SAP = square antiprism and BCTP = bicapped trigonal prism.

mean Yb—N bond length can be compared with the values of 2.47 for $[Yb\{HB(pz)_3\}_3]$ [range: 2.401(8)–2.601(6) Å], 2.49 [ranges: molecule 1, 2.444(10)–2.576(11); molecule 2, 2.432(14)–2.526(13) Å] for $[Yb\{HB(pz)_3\}_2(acac)]$[11] and 2.48 Å [range: 2.425(12)–2.548(10) Å] for $[Yb\{HB(pz)_3\}_2(O_2C_7H_5)]$.[13b]

The structures of $[Yb\{B(pz)_4\}_3]$ and $[Yb\{HB(pz)_3\}_3]$ are similar in terms of arrangement of ligands around the ytterbium ion and coordination geometry. For $[Yb\{B(pz)_4\}_3]$, one of the two uncoordinated pyrazolyl rings [N(12)] of the bidentate ligand is pointed away from the metal and is on the plane of symmetry of the molecule;

Table 5. Selected bond distances (Å) and angles (°) for $[Yb\{B(pz)_4\}_3]^a$

Yb—N(1)	2.590(9)	Yb—N(6)	2.379(8)
Yb—N(2)	2.446(8)	Yb—N(7)	2.419(8)
Yb—N(3)	2.444(8)	Yb—N(9)	2.436(8)
Yb—N(5)	2.596(9)	Yb—N(10)	2.441(8)
B—N	1.54(2)	N—C	1.34(1)
N—N	1.37(1)	C—C	1.37(2)

N(2)—Yb—N(9)	74.4(3)	N(3)—Yb—N(10)	76.2(3)
N(2)—Yb—N(7)	86.7(3)	N(3)—Yb—N(6)	90.2(3)
N(7)—Yb—N(9)	92.2(3)	N(6)—Yb—N(10)	86.5(3)
N(6)—Yb—N(7)	81.4(3)	N(9)—Yb—N(10)	73.5(3)
N(2)—Yb—N(3)	77.7(3)	N(1)—Yb—N(5)	128.1(3)
N(1)—Yb—N(2)	71.6(3)	N(5)—Yb—N(6)	69.9(3)
N(1)—Yb—N(3)	71.1(3)	N(5)—Yb—N(7)	70.4(3)
N(1)—Yb—N(6)	71.1(3)	N(5)—Yb—N(9)	71.6(3)
N(1)—Yb—N(7)	71.0(3)	N(5)—Yb—N(10)	69.1(3)

[a] The average B—N, N—N, N—C and C—C lengths are given.

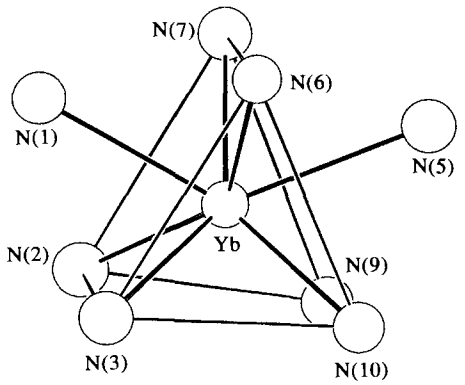

Fig. 5. BCTP coordination polyhedron of $[Yb\{B(pz)_4\}_3]$.

the other one [N(13)] is almost perpendicular to the plane of symmetry of the molecule, being too far from the metal to coordinate to the uncapped rectangular face to form a nine-coordinate tricapped trigonal prism.

The mean bite distance between the coordinated nitrogen atoms of the bidentate $[B(pz)_4]^-$ ligand is 2.97 Å compared with 3.00 Å in $[Yb\{HB(pz)_3\}_3]$, while for the bidentate ligand the bite distance is 2.92 Å compared with 3.00 Å in the same compound.

There are a few short intraligand contacts indicating a large steric crowding around the metal centre.

Supplementary material available. Tables of positional parameters, thermal parameters, calculated hydrogen atom positions, complete bond distances and angles, equations of mean-least squares and edge lengths of BCTP polyhedra (14 pages). Ordering information is given on any current masthead page.

Acknowledgement—The financial support of Fapesp, CNPq and Capes (Brazil) and JNICT (Portugal) is gratefully acknowledged.

REFERENCES

1. K. W. Bagnall, A. C. Tempest, J. Takats and A. P. Masino, *Inorg. Nucl. Chem. Lett.* 1976, **12**, 555.
2. M. V. R. Stainer and J. Takats, *Inorg. Chem.* 1982, **21**, 4050.
3. M. V. R. Stainer and J. Takats, *J. Am. Chem. Soc.* 1983, **105**, 410.
4. A. Seminara and A. Musumeci, *Inorg. Chim. Acta* 1984, **95**, 291.
5. R. A. Faltynek, *J. Coord. Chem.* 1989, **20**, 73.
6. W. D. Moffat, M. V. R. Stainer and J. Takats, *Inorg. Chim. Acta* 1987, **139**, 75.
7. D. L. Reger, J. A. Lindeman and L. Lebioda, *Inorg. Chim. Acta* 1987, **139**, 71.
8. D. L. Reger, J. A. Lindeman and L. Lebioda, *Inorg. Chem.* 1988, **27**, 3923.
9. D. L. Reger, S. J. Knox, J. A. Lindeman and L. Lebioda, *Inorg. Chem.* 1990, **29**, 416.
10. M. A. J. Moss and C. J. Jones, *Polyhedron* 1989, **8**, 1119.
11. (a) M. A. J. Moss, C. J. Jones and A. J. Edwards, *Polyhedron* 1988, **7**, 79; (b) M. A. J. Moss, C. J. Jones and A. J. Edwards, *J. Chem. Soc., Dalton Trans.* 1989, 1393.
12. M. A. J. Moss and C. J. Jones, *Polyhedron* 1990, **9**, 697.

13. (a) M. A. J. Moss and C. J. Jones, *Polyhedron* 1989, **8**, 555; (b) M. A. J. Moss and C. J. Jones, *J. Chem. Soc.* 1990, 581.
14. M. A. J. Moss and C. J. Jones, *Polyhedron* 1989, **8**, 2367.
15. M. A. J. Moss and C. J. Jones, *Polyhedron* 1989, **8**, 117.
16. F. T. Edelmann and U. Kilimann, *J. Organomet. Chem.* 1994, **469**, C5.
17. G. H. Maunder, A. Sella and D. A. Tocher, *J. Chem. Soc., Chem. Commun.* 1994, 885.
18. J. Takats, X. W. Zhang, V. W. Day and T. A. Eberspacher, *Organometallics* 1993, **12**, 4286.
19. D. L. Reger, J. A. Lindeman and L. Lebioda, *Inorg. Chem.* 1988, **27**, 1890.
20. A. Carvalho, A. Domingos, P. Gaspar, N. Marques, A. Pires de Matos and I. Santos, *Polyhedron* 1992, **11**, 1481.
21. D. L. Reger, Pi-Tai Chou, S. L. Studer, S. J. Knox, M. L. Martinez and W. E. Brewer, *Inorg. Chem.* 1991, **30**, 2397.
22. N. Marques and A. Pires de Matos, *Rare Earths' 92 in Kyoto* 1992, 236.
23. M. A. J. Moss, R. A. Kresinki, C. J. Jones and W. J. Evans, *Polyhedron* 1993, **12**, 1953.
24. R. McDonald, X. W. Zhang and J. Takats, 20th *Rare Earth Conference*, Monterey (1993).
25. L. Hasinoff, J. Takats, X. W. Zhang, A. H. Bond and R. D. Rogers, *J. Am. Chem. Soc.* 1994, **116**, 8833.
26. (a) H. Kagan, *Nouv. J. Chem.* 1990, **14**, 453; (b) W. J. Evans, *Polyhedron* 1987, **6**, 803.
27. S. Trofimenko, *J. Am. Chem. Soc.* 1967, **89**, 3170.
28. P. Girard, J. L. Namy and H. Kagan, *J. Am. Chem. Soc.* 1980, **102**, 2693.
29. C, H, and N analyses have been made but we were not able to obtain satisfactory results. However, mass spectra analyses and ^{1}H NMR spectra unambiguously identified the complexes.
30. A. Domingos, J. Marçalo, A. Paulo, A. Pires de Matos and I. Santos, *Inorg. Chem.* 1993, **32**, 5514.
31. P. C. Isolani and K. Zinner, *Quím. Nova* 1994, **17**, 65.
32. G. M. Sheldrick, SHELX Crystallographic Calculation Program. University of Cambridge, U.K. (1976).
33. G. M. Sheldrick, SHELX-93. University of Göttingen, Göttingen (1993).
34. International Tables for X-ray Crystallography, Vol. IV. Kinoch Press, Birmingham (1974).
35. A. Domingos, N. Marques and A. Pires de Matos, Latin-American Inorganic Chemistry Meeting, Santiago de Compostela (1993).
36. (a) S. Trofimenko, *J. Am. Chem. Soc.* 1967, **89**, 3170; (b) S. Trofimenko, *J. Am. Chem. Soc.* 1967, **89**, 6288; (c) S. Trofimenko, *J. Am. Chem. Soc.* 1969, **91**, 3183; (d) S. Trofimenko, *J. Am. Chem. Soc.* 1972, **94**, 5677; (e) D. L. Reger, S. S. Maso, A. L. Rheingold and R. L. Ostrander, *Inorg. Chem.* 1993, **32**, 5216.
37. (a) E. L. Muetterties and L. J. Guggenberger, *J. Am. Chem. Soc.* 1974, **96**, 1748; (b) M. G. B. Drew, *Coord. Chem. Rev.* 1979, **24**, 179.
38. W. J. Evans, J. W. Grate, H. W. Choi, I. Bloom, W. E. Hunter and J. L. Atwood, *J. Am. Chem. Soc.* 1985, **107**, 941.